

IC-Integrated Flexible Shear-Stress Sensor Skin

Yong Xu, Yu-Chong Tai, Adam Huang*, and Chih-Ming Ho*

MS 136-93, California Institute of Technology, Pasadena, CA 91125, USA

*MAE, University of California, Los Angeles, CA 90024, USA

ABSTRACT

This paper reports the first IC-integrated flexible shear-stress sensor skin. By integrating both bias and signal-conditioning circuitry on-chip, the wiring of the MEMS skin is significantly simplified and reliability is improved. The circuit is first made by a commercial IC foundry (i.e., Mitel) and micromachining is done on the CMOS wafers to form the skins. We further demonstrated the use of the sensor skin by packaging it on a semi-cylindrical aluminum block and tested it in a wind tunnel. In our experiment, the skin has successfully identified both the flow separation and stagnation points. It is believed that the IC-integrated smart skin technology demonstrated here can be applied to many other interesting applications in biomedicine, wearable microsystems, robotics and so on.

INTRODUCTION

Since the emergence of MEMS technology, numerous miniaturized sensors and actuators have been fabricated using techniques originally developed for the integrated circuits industry. Inherently, most MEMS devices are built on rigid substrates. However, for a wide variety of applications, it has long been desirable for sensors, actuators and circuits to be mounted on non-planar surfaces or even on flexible objects such as a human body. For example, we have been working on a new way of controlling the Unmanned Aerial Vehicle (UAV) through the sensing/controlling of the flow separation at the leading edge. This requires distributed sensors mounted on the cylindrical surface of leading edge. Accordingly, we developed flexible shear-stress sensor skins for the UAV project [1]. These skins, however, contained only sensors and required many electrical lead connections. The complete separation-detecting system consisted of the packaged sensor skins, bias board, and data acquisition board and a tremendous number of interconnection cables as shown in Fig. 1.

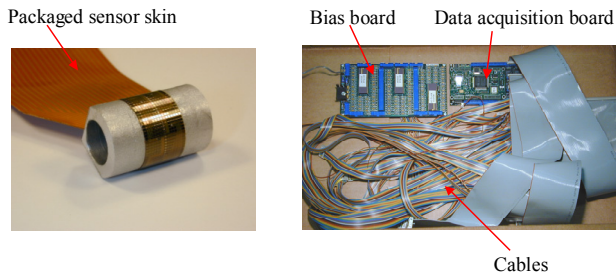


Figure 1 the flow separation detection system based on non-integrated sensor skin.

Therefore, it is highly desirable to develop IC-integrated shear-stress sensor skins with on-skin bias circuits, amplifiers, and multiplexers. By making IC-integrated skin, we can eliminate the bias board and interconnection cables, simplify the design of

the data acquisition board, and improve system reliability at the same time. However, the integration of MEMS and ICs onto the same flexible skin is a challenge.

Generally speaking, MEMS-IC integration can be categorized into two groups: hybrid integration and monolithic integration. In the case of hybrid integration, MEMS parts and circuit parts are fabricated separately and then are packaged together by wafer bonding or other packaging technologies. With regard to flexible shear-stress sensor skin, monolithic integration is preferred since hybrid integration does not simplify the packaging process. Based on when MEMS parts are fabricated, monolithic integration can be classified as mixed MEMS-IC process, MEMS-first process (pre-IC or pre-CMOS) and IC-first process (post-IC or post-CMOS). The first approach is best exemplified by Analog Devices' accelerometer, which is fabricated by interleaving and customizing the MEMS manufacturing steps with the IC process [2]. J. H. Smith et al. at Sandia National Laboratories developed a unique MEMS-first process [3]. In this approach, MEMS devices are first fabricated in a trench on the surface of the wafer. The wafer is then planarized and the trench is sealed. The wafer with MEMS is then processed using conventional process. However, it would be highly unlikely for any IC foundry service to modify their IC fabrication process or take pre-processed wafers. Therefore, most monolithic integration is done with the post-IC approach, taking advantages of the widely available CMOS foundry services. For this IC-integrated shear-stress sensor skin, post-CMOS process is chosen for the same reason.

DESIGN

The shear stress is of great importance for many applications such as fluid dynamics monitoring, but obtaining it remains a difficult task largely due to the lack of instrumentation. There are many methods to measure the local wall shear stress, including Stanton tube, direct measurement, thermal method, Preston tube, sub-layer fence and electrochemical technique [4]. Of these approaches, the thermal method is most widely used since it does not interfere with the flow and it offers the possibility of measuring time-varying flows. Conventional thermal shear-stress sensors are typically made by depositing thin-film metal resistors, mostly platinum or nickel, on flat substrates. During operation, the resistor is electrically heated, while the fluid flow cools it down. The input power of the resistor will change with the wall shear stress from the ambient flow field and this change can be readily detected electronically. A large portion of the power is lost to the substrate via thermal conduction. With micromachining technology, a vacuum cavity can be built underneath the resistor to reduce the heat loss to the substrate, thus improving the sensitivity and frequency response of sensor. The basic structure of the micromachined thermal shear stress sensor is a polysilicon resistor sitting on a nitride diaphragm with a vacuum cavity underneath [5, 6]. This is the sensor design used in the non-integrated sensor skin [1].

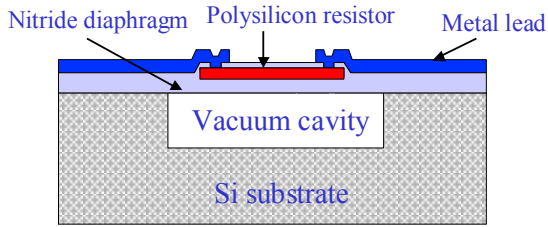


Figure 2 Cross-section of a vacuum insulated thermal shear stress sensor

Due to the limitation of post-CMOS process, this structure cannot be employed here. For this IC-integrated skin, the gate poly of the CMOS process is utilized as the sensing elements of the shear stress sensors. The silicon underneath is etched away to achieve the thermal isolation and a Parylene N layer is deposited as diaphragm. The cross section of the sensor is illustrated in Figure 5 (g).

Figure 3 shows the schematic of the integrated flexible shear-stress sensor skin. The shear-stress sensors, which utilize the gate polysilicon of the CMOS process as the sensing elements, operate in CC mode and are biased by the cascode current mirrors. The output voltage is multiplexed by PMOS switches and addressing circuitry. There are 16 shear stress sensors, which can be exactly accessed by a 4-bit address. An operational amplifier is also implemented to perform on-chip amplification.

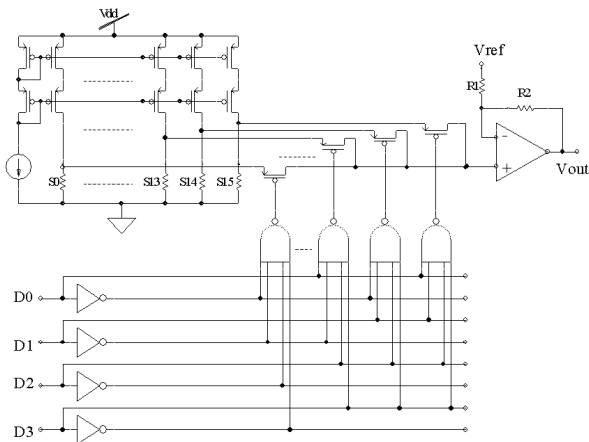


Figure 3 Schematic of the integrated flexible shear stress sensor skin.

FABRICATION

First, the circuits were fabricated by Mitel Semiconductor, which is Canadian CMOS foundry [7]. The gate poly of Mitel process is 320 nm thick, with a temperature coefficient of resistance (TCR) of 0.1% and a sheet resistance of 20Ω per square. Figure 4 shows the 6" wafer back from Mitel.

Then the post-CMOS process was conducted at the Caltech Micromachining Lab. Figure 5 (a) shows the cross section of the wafer back from Mitel. The polysilicon sensing elements are covered by dielectric and metal layers, so the process begins with patterning the metal and dielectric layers at the

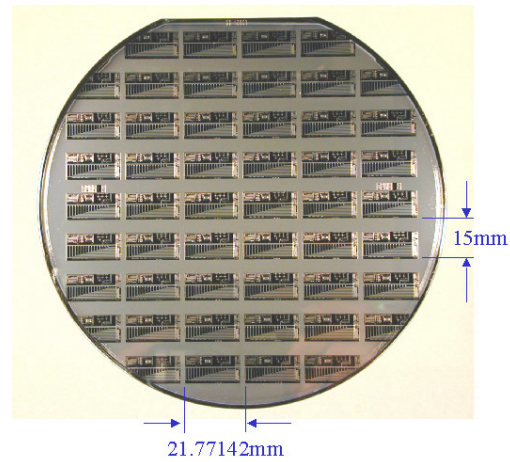


Figure 4 A 6" wafer back from Mitel.

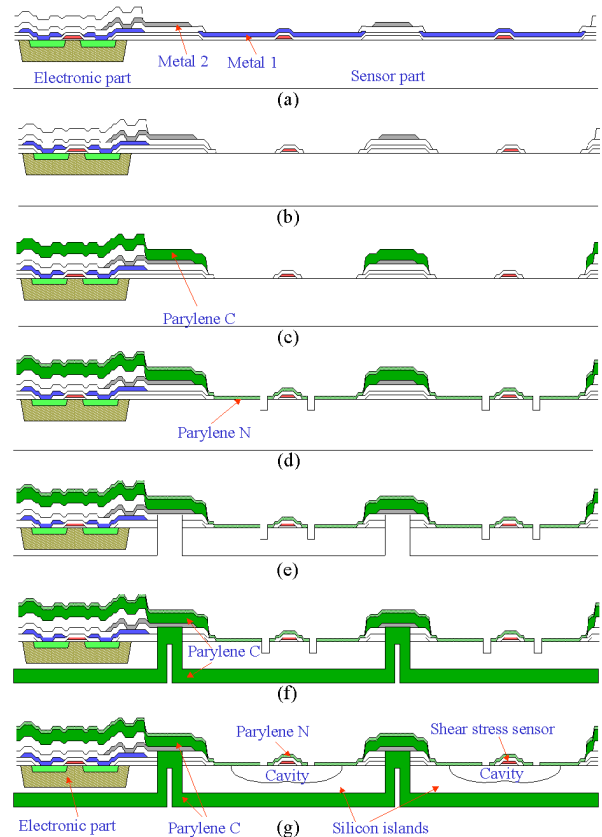


Figure 5 The simplified post-CMOS fabrication process.

sensor area, followed by deposition and patterning of 10 μm Parylene C on front side. Next, 1.5 μm Parylene N is deposited and patterned. Please note that both Parylene C and N are used in this project. Parylene C serves as the mechanical support to encapsulate the silicon islands while Parylene N serves as the diaphragm material to support the sensing element after releasing. There are two major differences between Parylene C and N which lead to their different roles. The first difference lies in the melting temperature. Parylene N has a much higher melting temperature (420 °C) than that of Parylene C (290 °C). Since the poly resistor will be heated up during operation, Parylene N is chosen as the membrane material to ensure the

high temperature compatibility. The second difference lies in the deposition rate. Parylene C has a much higher deposition rate than Parylene N. To provide enough mechanical support, we need approximately 10 μ m Parylene on both the front and back sides. It is impractical to deposit such a thick layer of Parylene N. The releasing holes for shear-stress sensor are then formed by patterning Parylene N as shown in Figure 5(d). These holes are further etched into the silicon substrate to enhance the BrF₃ releasing process.

The process at the backside begins with the thinning down of the wafer. Next the silicon islands are formed by dry etching from the back side. DRIE is used in these two steps. After etching silicon down to the dielectric layer on the front side, pad etchant is used to remove the dielectric layer. Now 10 μ m Parylene C is deposited on the wafer back side to sandwich the silicon islands. The final step is to release the polysilicon resistor by BrF₃ gas phase etching. The purpose of this step is to achieve good thermal isolation for the sensing element.

The integrated skin cut from the wafer is shown in Figure 6. The silicon islands are clearly seen by shining light from the backside. The metal leads going across the islands can also be clearly observed.

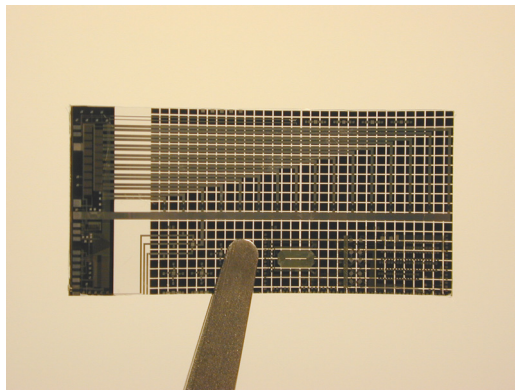


Figure 6 The fabricated IC-integrated skin held in tweezers.

PACKAGING

The sensor skin can be readily mounted on a non-planar surface. Figure 7 shows a single skin packaged on a semi-cylindrical surface of an aluminum block, which is the leading edge of an airfoil. Wire-bonding and conventional soldering were used to connect the sensor skin to the outside instrument. This configuration is adequate for our wind tunnel test. However, for real aircraft wing applications, the edge of the skin that contains the metal pads should be folded underneath the wing surface as in [1].

WIND TUNNEL TEST

The wind tunnel test was carried out in the UCLA wind tunnel lab. The testing set-up is illustrated in Figure 8. The integrated sensor skin was mounted on the top of the semi-cylindrical aluminum block. The definitions of sensor location θ and angle of attack α (AOA) can also be found in this figure. Shear stress distributions at different angles of attack were measured using the on-chip circuitry as shown in Figure 3. Sensor 0 is at the top surface and sensor 15 is at the bottom surface of the aluminum block. Since then angle between adjacent sensors is 12 $^\circ$ and the 16 sensors exactly span 180 $^\circ$. It is worth noting that the vertical

axis is the normalized output change $\Delta V/V$, where V is the output voltage. The purpose of this normalization is to minimize the non-uniformity of the sensors' shear-stress sensitivity caused by the process variation [8].

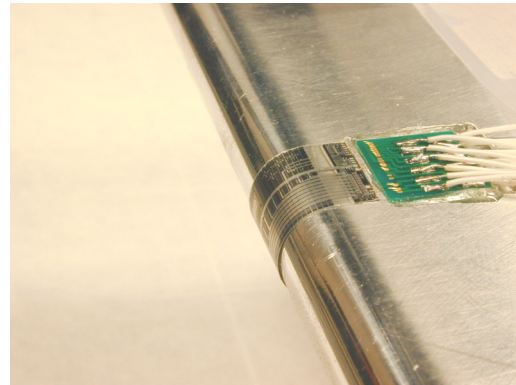


Figure 7 Sensor skins mounted on semi-cylindrical aluminum block

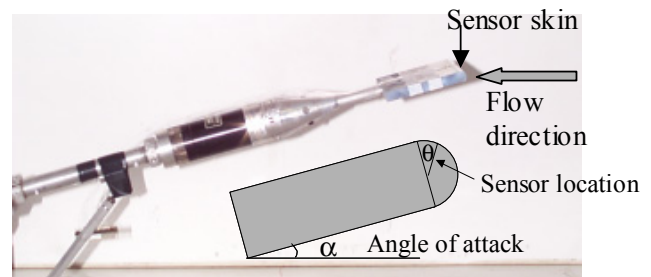
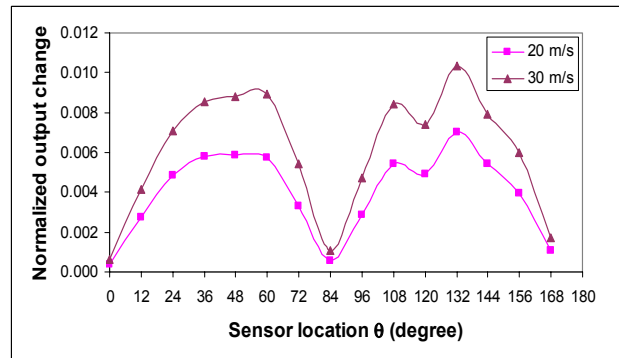
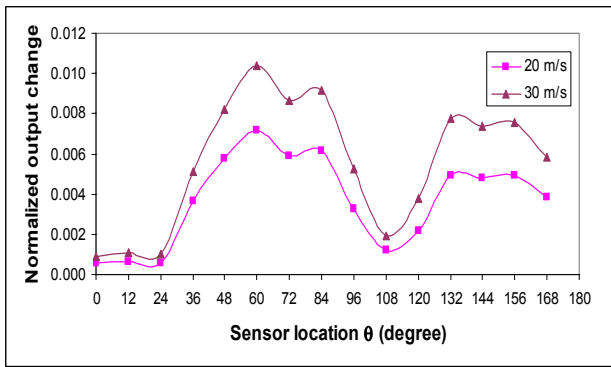


Figure 8 Testing setup in wind tunnel.

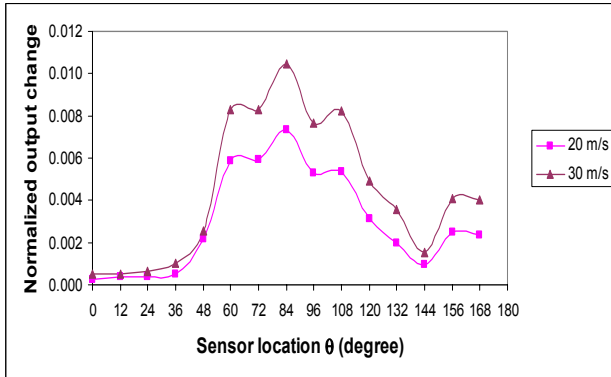
The separation point, which is characterized as the place where the shear stress has a sharp jump, can be clearly observed. Interestingly, the stagnation point, where the shear stress has a minimum value in the middle can also be identified. In the case of 0 $^\circ$ AOA, the stagnation point is at the sensor 7 (84 $^\circ$), which is exactly as expected. On the other hand, the separation points may be at sensor 0 and sensor 15 or even beyond. In the case of 15 $^\circ$ AOA, the separation point is at sensor 2 (24 $^\circ$) while the stagnation point is at sensor 9 (108 $^\circ$). For 30 $^\circ$ AOA, the separation point moves to sensor 3 (36 $^\circ$) while the stagnation point moves to sensor 12 (144 $^\circ$).



(a) 0 $^\circ$ angle of attack



(b) 15° angle of attack



(c) 30° angle of attack

Figure 9 Shear stress distributions at different angles of attack.

DISCUSSION

An IC-integrated shear-stress sensor skin is successfully fabricated. With bias and signal conditioning circuitry integrated on-chip, the packaging and deployment of the sensor skin are significantly simplified and the system reliability is improved. In the wind tunnel test, both separation and stagnation points are detected by the sensor skin.

The IC-integrated smart skin technology demonstrated in this paper may have many other interesting applications. The first example is for the biomedical applications. Many MEMS devices have already been widely employed in biomedicine where miniaturized sensors, actuators and other micro structures are needed. However, the IC-integrated smart skins can further promote us to another level of functionality. As shown in Figure 10, the sensor skin can be mounted on human body like a Band-Aid™. Examples for future applications may include smart skins with sensors capable of monitoring physiological parameters such as glucose and insulin levels. For implantable applications, sensors can be built on flexible substrates to conform to the organ shape or to minimize tissue trauma during patient movement. Smart skins incorporating arrays of tactile, temperature, and other sensors are very helpful to surgical instruments for minimally invasive surgery. The IC-integrated smart skin would also be of great promise for wearable microsystems, robotics and many other research areas.

ACKNOWLEDGEMENTS

This project is supported by DARPA under the Navy contract N66001-97-C-8610 and by the NSF Center for Neuromorphic

System Engineering at Caltech. Travel support has been generously provided by the Transducers Research Foundation and by the DARPA MEMS and DARPA BioFlips programs. The help from Justin Boland, Stacey Walker Boland, Matthieu Liger, Jun Xie and Trevor Roper is also highly appreciated.



Figure 10 Example of future applications of the smart skin technology.

REFERENCES

- [1] F. Jiang, Y. Xu, T. Weng, Z. Han, Y.-C. Tai, A. Huang, C.-M. Ho, and S. Newbern, "Flexible shear stress sensor skin for aerodynamics applications," presented at IEEE International Conference on Micro Electro Mechanical Systems (MEMS), Miyazaki, Japan, 2000.
- [2] W. Kuehnel and S. Sherman, "A Surface Micromachined Silicon Accelerometer with on-Chip Detection Circuitry," *Sensors and Actuators a-Physical*, vol. 45, pp. 7-16, 1994.
- [3] J. H. Smith, S. Montague, J. J. Sniegowski, J. R. Murray, and P. J. McWhorter, "Embedded micromechanical devices for the monolithic integration of MEMS with CMOS," presented at International Electron Devices Meeting. Technical Digest (Cat. No.95CH35810). IEEE. 1995, 1995.
- [4] T. J. Hanratty and J. A. Campbell, "Measurement of wall shear stress," in *Fluid Mechanics Measurements*, R. J. Goldstein, Ed., 2nd ed: Taylor & Francis, 1996, pp. 575-648.
- [5] C. Liu, Y. C. Tai, J. B. Huang, and C. M. Ho, "Surface Micromachined Thermal Shear Stress Sensor," presented at ASME International Mechanical Engineering Congress and Exposition, Chicago, IL, 1994.
- [6] Y. Xu, F. Jiang, Q. Lin, J. Clendenen, S. Tung, and Y.-C. Tai, "Underwater Shear-Stress Sensor," presented at IEEE International Conference on Micro Electro Mechanical Systems (MEMS), Las Vegas, Nevada, 2002.
- [7] "<http://www.mitelsemi.com>,".
- [8] Q. Lin, F. Jiang, X. Wang, Z. Han, Y. C. Tai, J. Lew, and C. M. Ho, "MEMS Thermal Shear-Stress Sensors: Experiments, Theory and Modeling," presented at Solid-State Sensor and Actuator Workshop, Hilton Head Island, SC, 2000.